

Modeling and Design of Rectangular Microstrip Patch Antenna with Iso/Anisotropic Substrate Using Neuro-spectral Computation Approach

Siham BENKOUDA, Sami BEDRA
Electronics Department, University of Batna.
Batna, 05000, Algeria.
bedra_sami@yahoo.fr

Imad BENACER, Tarek FORTAKI
Electronics Department, University of Batna.
Batna, 05000, Algeria.
t_fortaki@yahoo.fr

Abstract— In this paper, we propose a general design of rectangular microstrip antenna printed on isotropic or anisotropic substrate, based on artificial neural networks (ANN) in conjunction with spectral domain formulation. In the design procedure, syntheses ANN model is used as feed forward network to determine the resonant frequency. Analysis ANN model is used as the reversed of the problem to calculate the antenna dimension for the given resonant frequency, dielectric constant and height of substrate. The electromagnetic knowledge combined with artificial neural network in the analysis and the design of circular antenna to reduce the complexity of the spectral approach and to minimize the CPU time necessary to obtain the numerical results. The results obtained from the neural models are in very good agreement with the experimental results available in the literature.

Keywords- Rectangular Microstrip Antenna; Artificial Neural Network; design and modeling; spectral domain analysis; HFSS.

I. INTRODUCTION

The increase in complexity of device modeling has led to rapid growth in the computational modeling research arena. To accommodate computational complexity, several Computer Aided Design (CAD) modeling engines such as Artificial Neural Networks (ANNs) were used [1, 2]. ANNs, emulators of biological neural networks, have emerged as intelligent and powerful tools and have been widely used in signal processing, pattern recognition, and several other applications [3]. ANN is a massively parallel and distributed system traditionally used to solve problems of nonlinear computing [4].

The microstrip antenna (MSA) is an excellent radiator for many applications such as mobile antenna, aircraft and ship antennas, remote sensing, missiles and satellite communications [5]. It consists of radiating elements (patches) photo etched on the dielectric substrate. Microstrip antennas are low profile conformal configurations. They are light weight, simple and inexpensive, most suited for aerospace and mobile communication. Their low power handling capability posits these antennas better in low power transmission and receiving applications [6]. The flexibility of the Microstrip antenna to shape it in multiple ways, like square, rectangular, circular, elliptical, triangular shapes etc., is an added property.

Some dielectric substances exhibit anisotropy due to their natural crystal structures or as the result of their production processes [7]. Isotropic substances may also exhibit anisotropy at high frequencies. In the design of microwave integrated circuit components and microstrip patch antennas, anisotropic substances have been increasingly popular. Especially the effects of uniaxial type anisotropy have been investigated [7-11] due to availability of this type of substances such as Sapphire, Magnesium fluoride and Epsilam-10. In these works, the physical parameters of the antenna are replaced with effective ones in order to line up the obtained theoretical results with the measured data. Although the moment method provides better accuracy but its computational cost is high due to the evaluation of the slowly decaying integrals and the iterative nature of the solution process. Even though all the losses can be directly included in the analysis, produced results may not provide satisfactory accuracy for all the cases [12].

The objective of this work is to present an integrated approach based on artificial neural networks and electromagnetic knowledge. We introduce the artificial neural networks in the analysis of rectangular antenna to reduce the complexity of the spectral approach and to minimize the CPU time necessary to obtain the numerical results. Two points are especially emphasized: we have demonstrated the force of neurospectral approach in antenna modeling using ANN combined with electromagnetic (EM) knowledge to develop a neural network model for the calculation of resonant frequency of rectangular patch antenna printed on isotropic or uniaxially anisotropic substrate. Using reverse modeling, ANN is built to find out the antenna dimensions for the given resonant frequency, dielectric constant and height of substrate. The models are simple, easy to apply, and very useful for antenna engineers to predict both patch dimensions and resonant frequency. To the best of our knowledge, this subject has not been reported in the open literature; the only published results on analysis of rectangular microstrip-patch resonators on isotropic substrate using neurospectral approach [13-16].

II. FORMULATION OF THE PROBLEM

The geometry under consideration is illustrated in Figure 1. A rectangular patch with dimensions (a, b) along the two axes (x, y) , respectively, is printed on a grounded dielectric slab of thickness d , characterized by the free-space permeability μ_0 and the permittivity ϵ_0, ϵ_r (ϵ_0 is the free-space

permittivity and the relative permittivity ϵ_r can be complex to account for dielectric loss).

All fields and currents are time harmonic with the time dependence suppressed. The transverse fields inside the j th layer ($j = 1, 2$) can be obtained via the inverse vector Fourier transform as [17].

Figure1. rectangular microstrip antenna structure.

$$\mathbf{E}(\mathbf{r}_s, z) = \begin{bmatrix} E_x(\mathbf{r}_s, z) \\ E_y(\mathbf{r}_s, z) \end{bmatrix} = \frac{1}{4\pi^2} \int_{-\infty}^{+\infty} \int_{-\infty}^{+\infty} \bar{\mathbf{F}}(\mathbf{k}_s, \mathbf{r}_s) \cdot \mathbf{e}(\mathbf{k}_s, z) dk_x dk_y \quad (1)$$

$$\mathbf{H}(\mathbf{r}_s, z) = \begin{bmatrix} H_y(\mathbf{r}_s, z) \\ -H_x(\mathbf{r}_s, z) \end{bmatrix} = \frac{1}{4\pi^2} \int_{-\infty}^{+\infty} \int_{-\infty}^{+\infty} \bar{\mathbf{F}}(\mathbf{k}_s, \mathbf{r}_s) \cdot \mathbf{h}(\mathbf{k}_s, z) dk_x dk_y \quad (2)$$

where $\bar{\mathbf{F}}(\mathbf{k}_s, \mathbf{r}_s)$ is the kernel of the vector Fourier transform [18, 19], and

$$\mathbf{e}(\mathbf{k}_s, z) = \begin{bmatrix} i \frac{\partial \tilde{E}_z(\mathbf{k}_s, z)}{\partial z} \\ \mathbf{k}_s \\ \frac{\omega \mu_0}{k_s} \tilde{H}_z(\mathbf{k}_s, z) \end{bmatrix} = \mathbf{A}(\mathbf{k}_s) e^{-i\bar{k}_z z} + \mathbf{B}(\mathbf{k}_s) e^{i\bar{k}_z z} \quad (3)$$

$$\mathbf{h}(\mathbf{k}_s, z) = \begin{bmatrix} \frac{\omega \epsilon_0 \epsilon_r}{k_s} \tilde{E}_z(\mathbf{k}_s, z) \\ i \frac{\partial \tilde{H}_z(\mathbf{k}_s, z)}{\partial z} \\ \mathbf{k}_s \end{bmatrix} = \bar{\mathbf{g}}(\mathbf{k}_s) \cdot \left[\mathbf{A}(\mathbf{k}_s) e^{-i\bar{k}_z z} - \mathbf{B}(\mathbf{k}_s) e^{i\bar{k}_z z} \right] \quad (4)$$

In Eqs. 4 and 5, $\tilde{E}_z(\mathbf{k}_s, z)$ and $\tilde{H}_z(\mathbf{k}_s, z)$ are the scalar Fourier transforms of $E_z(\mathbf{r}_s, z)$ and $H_z(\mathbf{r}_s, z)$, respectively. \mathbf{A} and \mathbf{B} are two-component unknown vectors and

$$\bar{\mathbf{g}}_j(\mathbf{k}_s) = \text{diag} \left[\frac{\omega \epsilon_0 \epsilon_{rj}}{k_z}, \frac{k_z}{\omega \mu_0} \right] \quad (5)$$

$$k_z = (\epsilon_r k_0^2 - \mathbf{k}_s^2)$$

with $k_0^2 = \omega^2 \epsilon_0 \mu_0$ and k_z is the propagation constant in the uniaxial substrate. Writing Eqs. 4 and 5 in the planes $z=0$ and $z=d$, and by eliminating the unknowns \mathbf{A} and \mathbf{B} , we obtain the matrix form

$$\begin{bmatrix} \mathbf{e}(\mathbf{k}_s, d^-) \\ \mathbf{h}(\mathbf{k}_s, d^-) \end{bmatrix} = \bar{\mathbf{T}} \cdot \begin{bmatrix} \mathbf{e}(\mathbf{k}_s, 0^+) \\ \mathbf{h}(\mathbf{k}_s, 0^+) \end{bmatrix} \quad (6)$$

with

$$\bar{\mathbf{T}} = \begin{bmatrix} \bar{\mathbf{T}}^{11} & \bar{\mathbf{T}}^{12} \\ \bar{\mathbf{T}}^{21} & \bar{\mathbf{T}}^{22} \end{bmatrix} = \begin{bmatrix} \bar{\mathbf{I}} \cos \bar{\theta} & -i \bar{\mathbf{g}}^{-1} \sin \bar{\theta} \\ -i \bar{\mathbf{g}} \sin \bar{\theta} & \bar{\mathbf{I}} \cos \bar{\theta} \end{bmatrix} \quad (7)$$

which combines \mathbf{e} and \mathbf{h} on both sides of the j th layer as input and output quantities. In Eq. 8, $\bar{\theta} = \mathbf{k}_z d$. Now that we have the matrix representation of the anisotropic substrate characterized by the permittivity tensor, it is easy to derive the dyadic Green's function of the problem in a manner very similar to that shown in [9]

$$\mathbf{e}(\mathbf{k}_s, d^-) = \mathbf{e}(\mathbf{k}_s, d^+) = \mathbf{e}(\mathbf{k}_s, d) \quad (8)$$

$$\mathbf{h}(\mathbf{k}_s, d^-) = \mathbf{h}(\mathbf{k}_s, d^+) = \mathbf{j}(\mathbf{k}_s) \quad (9)$$

$\tilde{\mathbf{J}}(\mathbf{k}_s)$ is the vector Fourier transform of current $\tilde{\mathbf{J}}(\mathbf{r}_s)$ on the patch, it accounts for the discontinuity of the tangential magnetic field at the interface $z=d$. In the unbounded air region above the top patch of the structure ($d < z < \infty$ and $\epsilon_r = 1$) the electromagnetic field given by Eqs. 3 and 4 should vanish at $z \rightarrow +\infty$ according to Sommerfeld's condition of radiation, this yields

$$\mathbf{h}(\mathbf{k}_s, d^+) = \bar{\mathbf{g}}_0(\mathbf{k}_s) \cdot \mathbf{e}(\mathbf{k}_s, d^+) \quad (10)$$

$$\mathbf{h}(\mathbf{k}_s, 0^-) = -\bar{\mathbf{g}}_0(\mathbf{k}_s) \cdot \mathbf{e}(\mathbf{k}_s, 0^-) \quad (11)$$

where $\bar{\mathbf{g}}_0(\mathbf{k}_s)$ can be easily obtained from the expression of $\bar{\mathbf{g}}_j(\mathbf{k}_s)$ given in Eq. 5 by allowing $\bar{\epsilon}_r = 1$. The transverse electric field must necessarily be zero at the plane $z = 0$, so that we have

$$\mathbf{e}(\mathbf{k}_s, d^-) = \mathbf{e}(\mathbf{k}_s, d^+) = \mathbf{e}(\mathbf{k}_s, d) = 0 \quad (12)$$

From Eqs. 6-11, we obtain the following relationship:

$$\mathbf{e}(\mathbf{k}_s, d) = \bar{\mathbf{G}}(\mathbf{k}_s) \cdot \mathbf{j}(\mathbf{k}_s) \quad (13)$$

Where $\bar{\mathbf{G}}(\mathbf{k}_s)$ is the dyadic Green's function in the vector Fourier transform domain, it is given by

$$\bar{\mathbf{G}}(\mathbf{k}_s) = \begin{bmatrix} \bar{\mathbf{T}}_1^{22} (\bar{\mathbf{T}}_1^{12})^{-1} + (\bar{\mathbf{g}}_0 \cdot \bar{\mathbf{T}}_2^{12} - \bar{\mathbf{T}}_2^{22})^{-1} \\ + (\bar{\mathbf{g}}_0 \cdot \bar{\mathbf{T}}_1^{11} - \bar{\mathbf{T}}_1^{21})^{-1} \end{bmatrix}^{-1} \quad (14)$$

Using the technique known as the moment method, with weighting modes chosen identical to the expansion modes, Eqs. 12 and 13 are reduced to a system of linear equations which can be written compactly in matrix form [18] as

$$\bar{\mathbf{Z}} \cdot \mathbf{C} = \mathbf{0} \quad (15)$$

where $\bar{\mathbf{Z}}$ is the impedance matrix and the elements of the vector \mathbf{C} are the mode expansion coefficients to be sought [18, 19]. Note that each element of the impedance matrix $\bar{\mathbf{Z}}$ is expressed in terms of a doubly infinite integral [18]. The system of linear equations given in Eq. 16 has non-trivial solutions when

$$\det [\bar{\mathbf{Z}}(\omega)] = 0 \quad (16)$$

Although the full-wave analysis can give results for several resonant modes [18, 19], only results for the TM_0 mode are presented in this study.

If we want to take the substrate uniaxial anisotropy into account, the number of inputs increases; since the relative dielectric permittivity ϵ_r will be replaced by the pair of relative permittivities (ϵ_x, ϵ_z) , where ϵ_x and ϵ_z are the relative dielectric permittivity along x and z axis, respectively (Fig. 1). With the increase of design parameters number, the network size increases, resulting in an increase in the size of training set required for proper generalization. Because of the different natures of the additional parameters, data generation becomes more complicated, a solution to this problem seems necessary. For the case of uniaxially anisotropic substrate, ϵ_r given in [20] there resulting values are:

$$\epsilon_{re} = \epsilon_z \quad (17)$$

$$d_e = d \cdot \frac{\epsilon_x}{\epsilon_z} \quad (18)$$

In the following section, a basic artificial neural network is described briefly and our application to the calculation of the resonant frequency of a microstrip antenna is then explained.

III. ARTIFICIAL NEURAL NETWORKS

A. Multilayer Perceptron (MLP) networks

The ANN represents a promising modeling technique, especially for data sets having nonlinear relationships that are frequently encountered in engineering [20-22]. In the course of developing an ANN model, the architecture of the neural network and the learning algorithm are the two most important factors. ANNs have many structures and architectures [20, 21]. The class of the ANN and/or the architecture selected for a particular model implementation depends on the problem to be solved. After several experiments using different architectures coupled with different learning algorithms, in this paper the MLP neural-network architecture is used in the calculation of the input resistance of rectangular MSAs.

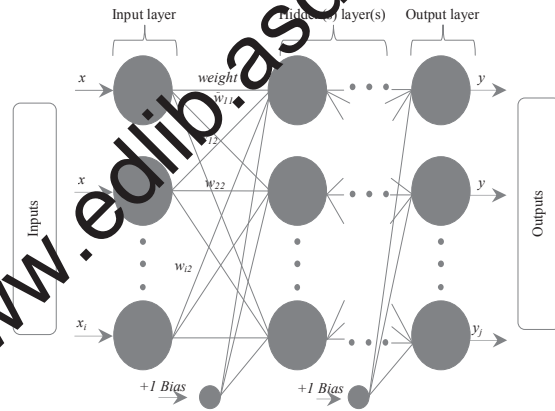


Figure 2. General form of multilayered perceptrons.

Multilayer perceptrons (MLPs) [23], which are among the simplest and therefore most commonly used neural network architectures, have been adapted for the calculation of the resonant frequency. MLPs can be trained with the use of many different algorithms. In this work, the standard back-propagation algorithm has been used for training MLP.

As shown in Fig. 2, the MLP consists of an input layer, one or more hidden layers, and an output layer. Neurons in the input layer only act as buffers for distributing the input signals x_i to neurons in the hidden layer. Each neuron in the hidden layer sums its input signals x_i after weighting them with the strengths of the respective connections w_{ji} from the input layer and computes its output y_j as a function f of the sum, namely

$$y_j = f(\sum w_{ji} x_i), \quad (19)$$

Where f can be a simple threshold function or a sigmoid or hyperbolic tangent function. The output of neurons in the output layer is computed similarly.

Training of a network is accomplished through adjustment of the weights to give the desired response via the learning algorithms. An appropriate structure may still fail to give a better model unless the structure is trained by a

suitable learning algorithm. A learning algorithm gives the change $\Delta w_{ji}(k)$ in the weight of a connection between neurons i and j at time k . The weights are then updated according to the formula

$$w_{ji}(k+1) = w_{ji}(k) + \Delta w_{ji}(k+1) \quad (20)$$

In this work, both Multilayer Perceptron (MLP) networks are used in ANN models. The structures of these ANNs are described briefly below.

B. Structures of the Neural Networks

In this work, both Multilayer Perceptron (MLP) networks were used in ANN models. MLP models were trained with almost all network learning algorithms. Hyperbolic tangent sigmoid and linear transfer functions were used in MLP training. The train and test data of the synthesis and analysis ANN were obtained from calculated with spectral model and a computer program using formulae given in Section 2. The data are in a matrix form consisting inputs and target values and arranged according to the definitions of the problems. Using [20, 21], two are generated for learning and testing the neural model. The different network input and output parameters are shown in Figure 3 and 4. As it is shown in this figure, the EM knowledge in form of empirical functions, given by (17) and (18) for the case of uniaxial anisotropic substrate, is used to preprocess the ANN model inputs. Some strategies are adopted to reduce time of training and ameliorate the ANN model accuracy, such as preprocessing of inputs and output, randomizing the distribution of the learning data [20-25], and resampling with a smaller discretization step in the part of input space corresponding to an unacceptably high error (small antenna parameters give large variation in the resonant frequency). All of the results presented in the paper were obtained on a Pentium IV computer with a 2.6-GHz processor and a total RAM memory of 2 GB.

In this work, the patch geometry of the microstrip antenna is obtained as a function of input variables, which are height of the dielectric material (d_e), dielectric constants of the substrate (ϵ_{re}), and the resonant frequency (f_r), using ANN techniques “Fig. 3”. Similarly, in the analysis ANN, the resonant frequency of the antenna is obtained as a function of patch dimensions (W), height of the dielectric substrate (d_e), and dielectric constants of the material (ϵ_{re}) “Fig. 4”. Thus, the forward and reverse sides of the problem will be defined for the circular patch geometry in the following subsections.

IV. APPLYING THE NEURO-COMPUTATIONAL TECHNIQUE

Synthesis of the patch geometry of the microstrip antenna is a problem for which closed-form solutions exist. Therefore, this example is very useful for illustrating features and capabilities of synthesis ANN. Details of the problem are presented next.

A. The forward side of the problem: The synthesis ANN

The input quantities to the ANN black-box in synthesis “Fig. 3” can be ordered as:

- d_e : height of the dielectric substrate;
- ϵ_{re} : effective dielectric substrate;
- f_r : resonant frequency of the antenna.

The following quantities can be obtained from the output of the black-box as functions of the input variables:

- W : width of a rectangular patch;
- L : length of a rectangular patch.

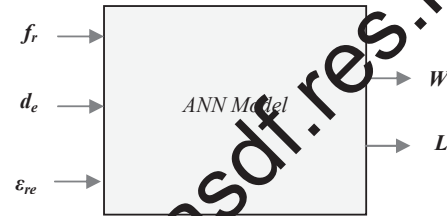


Figure 3. Synthesis Neural model for predicting the patch geometry of rectangular microstrip antenna with effective parameters.

B. The reverse side of the problem: The analysis ANN

In the analysis side of the problem, terminology similar to that in the synthesis mechanism is used, but the resonant frequency of the antenna is obtained from the output for a certain dielectric substrate and patch dimensions at the input as shown in “Fig. 4”

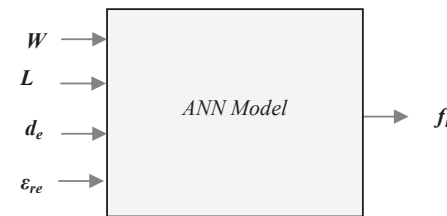


Figure 4. Analysis Neural model for calculating the resonant frequency of rectangular microstrip antenna with effective parameters.

The details of the network parameters for both these cases (analysis and synthesis) model are given in Table I.

TABLE I. COMPARISON OF PERFORMANCE DETAILS OF ANALYSIS AND SYNTHESIS MODEL.

| Algorithm details | Neurospectral approach | |
|--------------------------------------|------------------------|------------------|
| | Analysis model | Synthesis model |
| Activation function | sigmoid | sigmoid |
| Training function (back-propagation) | trainrp | trainrp |
| Number of data | 180 | 180 |
| Number of neurons (input layer) | 4 | 3 |
| Number of neurons (hidden layers) | 12-8 | 8-8 |
| Number of neurons (output layer) | 1 | 2 |
| Epochs (number of iterations) | 20000 | 50000 |
| TPE (training performance error) | 10 ⁻⁴ | 10 ⁻⁴ |
| Time required | 32 min | 56 min |
| LR (learning rate) | 0.6 | 0.5 |
| MC (momentum constant) | 0.1 | 0.1 |

V. NUMERICAL RESULTS AND DISCUSSION

In order to determine the most appropriate suggestion given in the literature, we compared our computed values of the resonant frequencies of rectangular patch antennas with the theoretical and experimental results reported by other scientists, which are all given in Table II.

TABLE II. ANALYSIS OF COMPUTED, MEASURED AND ANN PREDICTED RESONANT FREQUENCIES.

| Substrate material | Input parameters (cm) | | | Resonant frequencies (GHz) | | | |
|---|-----------------------|------|-------|----------------------------|--------|------|---------|
| | W | L | d | Measured | Theory | | Our ANN |
| | | | | [26] | [27] | [30] | |
| Isotropic (ε _x =ε _y =2.33) | 5.7 | 3.8 | 0.318 | 2.31 | 2.32 | 2.46 | 2.32 |
| | 2.95 | 1.95 | 0.318 | 4.24 | 4.18 | 4.34 | 4.28 |
| | 1.95 | 1.3 | 0.318 | 5.84 | 5.86 | 6.01 | 6.00 |
| | 1.4 | 0.9 | 0.318 | 7.70 | 7.73 | 7.79 | 7.69 |
| Anisotropic (ε _x , ε _y)=(13, 10.2) | W | L | d | Measured | Theory | | Our ANN |
| | | | | [28] | [28] | [29] | |
| | 3 | 2 | 0.127 | 2.26 | 2.26 | 2.23 | 2.23 |
| | 1.5 | 0.95 | 0.127 | 4.49 | 4.52 | 4.47 | 4.54 |
| | 3 | 1.9 | 0.254 | 2.24 | 2.26 | 2.24 | 2.22 |

Table III gives the antenna dimension calculated by the ANN model. As it is shown the resulting are in good agreement.

TABLE III. REVERSE MODELING FOR THE PREDICTION OF ANTENNA DIMENSIONS.

| Input parameters | | | Target (cm) | | ANN (cm) | |
|----------------------|--------|----------------|-------------|------|----------|-------|
| f _r (GHz) | d (cm) | ε _r | W | L | W | L |
| 3.92 | 0.079 | 2.22 | 4 | 2.5 | 3.989 | 2.512 |
| 4.30 | 0.127 | 10.5 | 1.5 | 1.1 | 1.508 | 1.091 |
| 4.73 | 0.9525 | 2.33 | 1.7 | 1.1 | 1.698 | 1.114 |
| 7.87 | 0.1524 | 2.33 | 1.7 | 1.1 | 1.701 | 1.098 |
| 2.31 | 0.3175 | 2.33 | 5.7 | 3.8 | 5.710 | 3.784 |
| 4.24 | 0.3175 | 2.33 | 2.95 | 1.95 | 2.951 | 1.948 |
| 5.84 | 0.3175 | 2.33 | 1.95 | 1.3 | 1.948 | 1.905 |
| 7.70 | 0.3175 | 2.33 | 1.4 | 0.9 | 1.397 | 0.953 |
| 2.264 | 0.127 | 10.2 | 3 | 2 | 3.008 | 1.998 |
| 4.495 | 0.127 | 10.2 | 1.5 | 0.95 | 1.485 | 0.953 |
| 2.242 | 0.254 | 10.2 | 3 | 1.9 | 3.008 | 1.907 |

It can be clearly seen from Tables II and III that our results calculated by using the neural model proposed in this paper are better than those computed by other scientists. The very good agreement between the measured values and our computed resonant frequency values supports the validity of the neural model even with the limited data set.

VI. CONCLUSION

A neural network-based CAD model can be developed for the design and analysis of a rectangular patch antenna, which is robust both from the angle of time of computation and accuracy. A distinct advantage of neuro-computing is that, after proper training, a neural network completely bypasses the repeated use of complex iterative processes for new cases presented to it. The single network structure can predict the results for patch antenna provided that input values are in the domain of training values. In the first example, a general design procedure for the microstrip antennas has been suggested using artificial neural networks and this is demonstrated using the rectangular patch

geometry. The spectral domain technique combined with the ANN method is several hundred times faster than the direct solution. This remarkable time gain makes the designing and training times negligible. Consequently, the Neur-spectral method presented is a useful method that can be integrated into a CAD tool, for the analysis, design, and optimization of practical shielded (Monolithic microwave integrated circuit) MMIC devices.

REFERENCES

- [1] K. R. Mishra, "Designing Rectangular Patch Antenna Using the Neurospectral Method" IEEE trans antenna and Propagat, VOL. 51, pp 1914-1921. 8, Aug 2003.
- [2] V.V. Thakare, P. Singhal; "Microstrip Antenna Design Using Artificial Neural Networks" Int J RF and Microwave CAE 20: 76-86, 2010.
- [3] D. Vijay, Lakshman M Srinivas, V. Vani Ch Yuriy G, Tayfun O "Sensitivity Driven Artificial Neural Network Correction Models for RF/Microwave Devices" Int J RF and Microwave CAE 22:30-40, 2012.
- [4] F. Wang, V.K. Devabhaktuni, and Q.J. Zhang, "Neural network structures and training algorithms for RF and micro-wave application" Int J RF Microwave Comput Aided Eng 9(1999), 216-240.
- [5] G. Kumar and K. P. Ray, "Broadband Microstrip Antennas "Artech House, London, 2003.
- [6] G. Garg, P. Bhartia, I. Bahl and A. Ittipiboon, "Microstrip Antenna Design Handbook," Artech House, Canton, 2001.
- [7] S. Gurel, and E. Yazgan, "Characteristics of a circular patch microstrip antenna on a uniaxially anisotropic substrate," IEEE Trans. Antennas Propagat., Vol. 52, No. 10, 2532-2537, 2004.
- [8] F. Bouttout, F. Benabdellaziz, A. Benghalia, D. Khedrouche, and T. Fortaki, "Uniaxially anisotropic substrate effects on resonance of rectangular microstrip patch antenna," Electron. Lett., Vol. 35, No. 4, 255-256, 1999.
- [9] T. Fortaki, and A. Benghalia, "Rigorous full-wave analysis of rectangular microstrip patches over ground planes with rectangular apertures in multilayered substrates that contain isotropic and uniaxial anisotropic materials," Microwave Opt. Technol. Lett., Vol. 41, No. 6, 496-500, 2004.
- [10] T. Fortaki, L. Djouane, F. Chebara, and A. Benghalia, "On the dual-frequency behavior of stacked microstrip patches," IEEE Antennas Wireless Propagat. Lett., Vol. 7, 310-313, 2008.
- [11] A. Boufrioua, and A. Benghalia, "Radiation and resonant frequency of a resistive patch and uniaxial anisotropic substrate with entire domain and ro of top functions," Engineering Analysis with Boundary Elements, Vol. 32, No. 7, 591-596, 2008.
- [12] T. Fortaki, D. Khedrouche, F. Bouttout and A. Benghalia, "Vector Hankel transform analysis of a tunable circular microstrip patch", Commun. Numer. Meth. Engng, 21:219-231, 2005.
- [13] R.K. Mishra, A. Patnaik, "Designing rectangular patch antenna using the neurospectral method", IEEE Transactions on Antennas and Propagation, Vol-51, Pp.1914 - 1921, Aug 2003.
- [14] R.K. Mishra, A. Patnaik, "Neurospectral analysis of coaxial fed rectangular patch antenna", Antennas and Propagation Society International Symposium, 2000. IEEE, 1062 - 1065 vol 2.
- [15] R.K. Mishra, A. Patnaik, "Neurospectral computation for input impedance of rectangular microstrip antenna", Electronics Letters, 30 Sep 1999, Vol-35, pp.1691 - 1693,
- [16] R.K. Mishra, A. Patnaik, "Neurospectral computation for complex resonant frequency of microstrip resonators", IEEE Microwave and Guided Wave Letters, VOL. 9, NO. 9, SEP 1999, pp.351-353.

- [17] D. M. Pozar, *Microwave Engineering*. (Addison-Wesley, Reading, Massachusetts, 1990), pp. 663-670.
- [18] T. Fortaki, L. Djouane, F. Chebara, and A. Benghalia, (2008), "Radiation of a rectangular microstrip patch antenna covered with a dielectric layer", *International Journal of Electronics*, 95:9, 989-998.
- [19] F. Bouttout, F. Benabdelaziz, T. Fortaki, and D. Khedrouche, "Resonant frequency and bandwidth of a superstrate loaded rectangular patch on a uniaxial anisotropic substrate", *Commun. Numer. Methods Eng.*, 2000, 16, (7), pp. 459-473.
- [20] Y. Tighilt, F. Bouttout, and A. Khellaf, "Modeling and design of printed antennas Using neural networks", *Int J RF and Microwave CAE* 21:228-233, 2011.
- [21] C. Christodoulou, and M. Georgiopoulos, "Applications of Neural Networks in Electromagnetics," Norwood, MA: Artechhouse, 2001.
- [22] A. Patnaik and R. K. Mishra, "ANN techniques in microwave engineering," *IEEE Micro*, vol. 1, pp. 55-60, Mar. 2000.
- [23] K. Guney and S. S. Gultekin, "A comparative study of neural networks for input resistance computation of electrically thin and thick rectangular microstrip antennas", *Journal of Communications Technology and Electronics*, 2007, Vol. 52, No. 5, pp. 483-492.
- [24] C. Christodoulou, and M. Georgiopoulos, "Applications of Neural Networks in Electromagnetics," Norwood, MA: Artechhouse, 2001.
- [25] Z. Raida, "Modeling EM structures in the neural network toolbox of MATLAB," *IEEE Antennas Propag Mag* 44, 2002, 46-67.
- [26] E. Chang, S.A. Long, and W.F. Richards, "Experimental investigation of electrically thick rectangular microstrip antennas", *IEEE Trans Antennas Propag.* Vol. 34, pp.767-772, 1986.
- [27] S. Chattopadhyay, M. Biswas, J. Y. Siddiqui, and D. Guha, "Rectangular microstrip with variable air gap and varying aspect ratio: Improved formulations and experiments", *Microwave Opt Technol Lett* 51: 169-173, 2009.
- [28] D. M. Pozar, "Radiation and scattering from a microstrip patch on a uniaxial substrate," *IEEE Trans. Antennas Propagation*, vol. 35, pp. 613-621, June 1987.
- [29] A. K. Verma, Nasimuddin, "Input impedance of rectangular microstrip patch antenna with iso/anisotropic substrate-superstrate", *IEEE Microwave and Wireless Components Letters*, Vol. 11, No. 11, pp. 456-458, Nov. 2001.
- [30] HFSS: High Frequency Structure Simulator, Ansoft Corp, Pittsburgh, PA.